Single-Phase to Three-phase Electrolytic Capacitor-Less Dual Inverter-Fed IPMSM for Suppress Torque Pulsation

Motoki Nishio, *Non-member* and Hitoshi Haga, *Member, IEEE*

***Abstract*— An electrolytic capacitor-less single-phase to three-phase power converter controls the motor and the input power factor. However, the motor power and the torque are pulsated because the input power of the inverter is irregular. This paper proposes a power converter and control method to realize a high input power factor and constant motor torque using a dual inverter without an electrolytic capacitor and an open-end winding machine. The proposed system has the following features. First, the proposed control method achieves a high input power factor by controlling the single-phase ac power without affecting the motor current. Second, the proposed control method compensates the pulsation the of load voltage by using an additional inverter. The proposed circuit configuration and control method contributes to the small size and weight, and high efficiency of the motor drive system with a single-phase power supply. The effectiveness of the proposed system is verified through experiments. The proposed system suppresses torque pulsation by 95.5% compared to the conventional system, and the input power factor is 97.2% at 1.5 Nm and 2500 rpm load condition.**

***Index Terms*—Dual inverter, electrolytic capacitor-less inverter, high power factor, open-end winding machine, torque pulsation suppression.**

I. INTRODUCTION

VARIABLE speed and high-efficiency single-phase ac motor systems have been used in home appliances to reduce energy consumption. In recent years, Power Factor Correction (PFC) circuits have been required for ac motor drive systems used in home appliances. The primary goal is to reduce harmonics distortion in the single-phase ac power supply side and improve transmission efficiency. Fig. 1 shows the conventional motor drive system that is composed of a PFC and a three-phase inverter. In [1]-[6], several conventional unidirectional boost-type PFC circuits are composed of boost inductors, low-side switches, and high-side diodes. Additionally, electrolytic capacitors are required in dc-link to smoothen the single-phase ac power. The electrolytic capacitors occupy a significant volume of the motor drive system. Furthermore, the lifespan of the whole system is shortened because of the susceptibility of electrolytic capacitors to heat. The inductors increase the power loss, the weight of the motor drive system, and its cost. PFC circuits are required to have high efficiency and small size and weight to save energy and resources of the motor drive system.

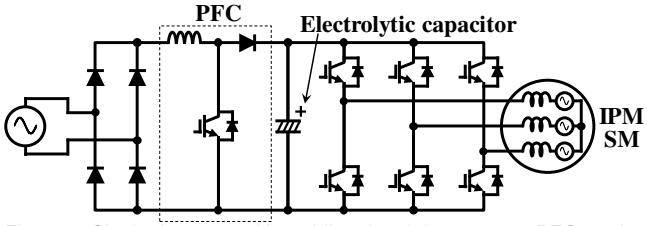

Fig. 1. Single inverter with unidirectional boost type PFC and an electrolytic capacitor.

In recent years, the Active Power Decoupling (APD) method that achieves the high input power factor, constant power supply, and high conversion efficiency without an electrolytic capacitor in the dc-link have been proposed [7]-[12]. In [7]-[10], a highly efficient motor drive has been achieved by using the small capacitance capacitor. However, the circuit size and the conversion loss increase because these circuits require an additional inductor. In [11], a switching device is added in series with the dc-link capacitor for constant power supply for the load motor. This circuit has a high power factor, low distortion of the input and output current; however, it limits the voltage utilization rate to less than a half and reduces the operating range of the load motor. Accordingly, a circuit that increases the voltage utilization rate is proposed in [12].

For these reasons, the Interior Permanent Magnet Synchronous Motor (IPMSM) drive system with a high-power factor diode rectifier circuit has been proposed in [13]-[17]. This system is effective as it has a low cost, long lifetime, small size and weight, because the PFC circuit, additional inductor, and electrolytic capacitor are not included. This system is used in home air-conditioners [17]. The conventional systems do not smoothen the single-phase ac power of the power supply using the power converter. Therefore, because the power converter has no energy storage element, single-phase power on the input side is supplied to the motor. The motor loss and mechanical noise are increased because the motor torque is pulsated with a 200% amplitude. Furthermore, since the upper limit of the

Manuscript received Jan. 07, 2020; revised April 07, 2020; accepted May 17, 2020.

M. Nishio and H. Haga are with Department of Electrical, Electronics and Information Engineering, Nagaoka University of Technology, Nagaoka, 940-2188, Japan (m_nishio@stn.nagaokaut.ac.jp, hagah@vos.nagaokaut.ac.jp)

output voltage of the inverter is low, there is also a challenge that the operational range of the load motor reduces. Furthermore, the motor copper loss increases because the peak value of the phase current increases. Therefore, the electrolytic capacitor-less inverter is effective in reducing the cost, extending the circuit life, and reducing the size and weight of the power converter. However, there are challenges in the load motor, such as increased mechanical vibration and noise caused by increasing the torque pulsation, a reduced operating range, and increased copper loss. Therefore, the application of the conventional system is limited to the compressor of the air-conditioner that can tolerate vibration and noise.

This paper proposes the configuration and control method of an electrolytic capacitor-less inverter using dual inverters and an open-end winding IPMSM. The proposed system drives an open-end winding IPMSM by two inverters, which have a small capacity film capacitor instead of an electrolytic one at each input. The proposed system does not require a large-capacity electrolytic capacitor and boost inductor. This study proposes the suppression of torque pulsation and power supply harmonics that occur at twice the power supply frequency. The proposed method in such a motor drive system is not shown. This paper proposes the circuit configuration and the control method to realize the suppression of the torque pulsation and power supply harmonics. The proposed system contributes to high efficiency, long lifetime and small circuit size and weight of the motor drive system with a single-phase ac power supply for home appliances. One of the inverters drives the motor and the pulsating single-phase ac power, while the other suppresses the load power pulsation. Another feature of the dual inverter is that the operating range of the motor is expanded. In [18]-[20], the operating range of the motor is increased by controlling the reactive power supplied to the motor in the dual inverter with an electrolytic capacitor. This paper presents an additional capacitor voltage control to support stable control, and input pulsation power control without pulsating torque. The effectiveness of the proposed system is shown by experimental results with an open-end winding IPMSM load. Moreover, this paper discusses the efficiency comparison between the single inverter without an electrolytic capacitor and the inverter composed of a PFC and an electrolytic capacitor that can achieve a high input power factor with a constant motor torque.

II. CIRCUIT TOPOLOGY

A. Conventional Electrolytic Capacitor-Less Single inverter

Fig. 2 shows the conventional electrolytic capacitor-less single inverter [13]-[17]. This conventional system consists of a single-phase diode rectifier, a small-capacity film capacitor at the dc-link, a voltage source inverter, and a Y-connected IPMSM at the load.

In a typical motor drive system, the input power is smoothed by a large-capacity electrolytic capacitor at the dc-link. However, the electrolytic capacitor-less inverter in Fig.2 has torque ripple because the dc-link capacitor is small-capacity

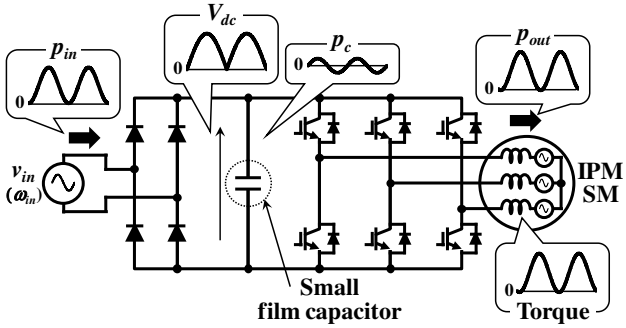

Fig. 2. Electrolytic capacitor-less single inverter.

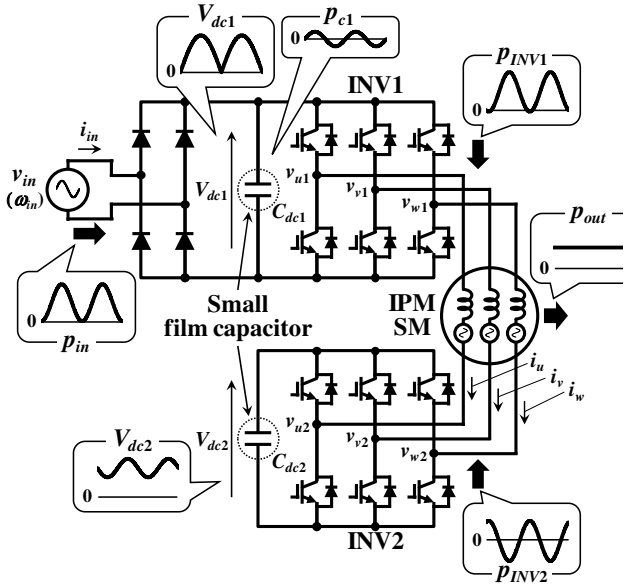

Fig. 3. Electrolytic capacitor-less dual inverter.

film capacitor. In the system of Fig. 2, the inverter can control the input power on the single-phase ac power supply side. The phase of the input current is matched with the input voltage when the phase of the single-phase ac power is matched with the input voltage. Therefore, the input power factor is approximately 1. A high input power factor is achieved without PFC by controlling the output power of the inverter to satisfy this condition. Therefore, the single-phase power is supplied to the load motor, directly. Motor q-axis current is varies in synchronization with the single-phase ac power to obtain a high input power factor. The inverter output power to obtain the high power factor is realized by controlling the motor current, which using the optimum switching pattern. In the system shown in Fig. 2, the torque ripple is smoothed by the inertia of the load motor. In the system shown in Fig. 2, the torque ripple of the motor is large, and the inverter output voltage also contains the ripple, which increases motor loss and noise.

B. Proposed Electrolytic Capacitor-Less Dual Inverter

Fig. 3 shows the proposed electrolytic capacitor-less dual inverter. The proposed system consists of a single-phase diode rectifier, two voltage source inverters with small-capacity film capacitors in the input, and an open-end winding IPMSM. The proposed system does not require a large-capacity electrolytic

TABLE I
PHASE VOLTAGE COMPARISON OF EACH SYSTEM

System	Phase voltage
Conventional system (Fig. 1 and 2)	$0, \pm\frac{1}{3}V_{dc}, \pm\frac{2}{3}V_{dc}$
Proposed system (Fig. 3)	$0, \pm\frac{1}{3}V_{dc1}, \pm\frac{2}{3}V_{dc1}, \pm\frac{1}{3}V_{dc2}, \pm\frac{2}{3}V_{dc2}, \pm\frac{1}{3}(V_{dc1} \pm V_{dc2}), \pm\frac{1}{3}(2V_{dc1} \pm V_{dc2}), \pm\frac{1}{3}(V_{dc1} \pm 2V_{dc2}), \pm\frac{2}{3}(V_{dc1} \pm V_{dc2})$

capacitor and boost inductor. The electrolytic capacitor and the boost inductor increase the cost and size of the system. However, semiconductors continue to evolve, and their cost and size continue to reduce. Therefore, the proposed system will be economically viable in the future. Furthermore, the open-end winding motor can continue operating using the other inverter even if the switching devices of one inverter fail. If the proposed system increases the reliability of the system, it is necessary to connect the dc parts of the two inverters through the relay. The effectiveness of the proposed system is limited to using the open-end winding motor for the load because the motor is required 6 terminals instead of 3 terminals.

In this paper, the power supply side inverter is expressed as INV1, the floating side inverter connected in series with INV1 through the load motor winding is expressed as INV2, the dc-link capacitor is expressed as C_{dc1}, and the floating capacitor is expressed as C_{dc2}.

In the proposed system, the output voltage difference between the inverters is supplied to the load. The phase voltage v_x ($x = u, v, w$) is written as follows:

$$v_x = v_{x1} - v_{x2}, \tag{1}$$

where v_{x1} and v_{x2} are the output voltages of each inverter. Table I shows the phase voltage generated based on the dc voltages V_{dc1} and V_{dc2} of INV1 and INV2 obtained from the (1). In the conventional single inverter, 5 levels of the phase voltage are applied to the motor by inverter switching. In the proposed dual inverter, 17 levels of the phase voltage are applied to the motor if the dc voltage is constant because the dc voltage of each inverter is at different potentials. The amount of change in the phase voltage decreases when the voltage applied to the motor becomes multi-level. Therefore, the voltage harmonics and motor iron loss are reduced by the dual inverter.

The relationship between the single-phase ac power p_{in}, the dc-link capacitor charging power p_{c1}, and the INV1 output power p_{INV1} is written as follows:

$$p_{in} = p_{c1} + p_{INV1}. \tag{2}$$

As shown in (2), p_{in} and p_{INV1} are not equal because of the existence of the dc-link capacitor charging power p_{c1}. Here, p_{c1} is written as follows:

$$\begin{aligned} p_{c1} &= v_{dc1} \times i_{dc1} \\ &= \frac{1}{2}\omega_{in} C_{dc1} V_{inm}{}^2 \sin(2\omega_{in} t), \end{aligned} \tag{3}$$

where v_{dc1} is the dc-link instantaneous voltage, V_{inm} is the dc-link maximum voltage, and ω_{in} is the single-phase power supply angular frequency.

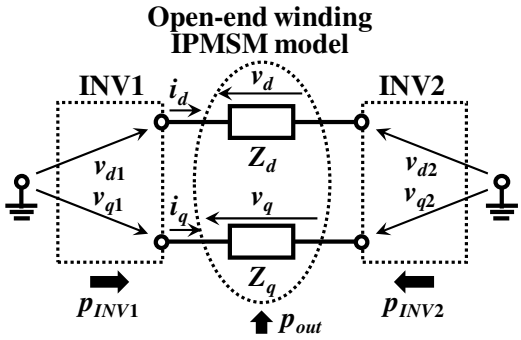

Fig. 4. Dual inverter power, dq-axis voltage and dq-axis current.

The relationship between the INV1 and INV2 output power p_{INV1}, p_{INV2}, and the load power p_{out} is written as follows:

$$p_{out} = p_{INV1} + p_{INV2}. \tag{4}$$

The output power is defined as the sum of the output power of INV1 and INV2.

Two inverters are connected in series through the stator winding of the load motor, as shown in Fig. 3. Therefore, a common current flows through each inverter. Furthermore, each output voltage is controlled independently. Fig. 4 shows the dq-axis model of the dual inverter. Here, Z_d and Z_q are dq-axis impedances of the open-end winding IPMSM, and the back-EMF is omitted in this model. The output power of INV1 is written as follows:

$$p_{INV1} = i_d v_{d1} + i_q v_{q1}, \tag{5}$$

where i_d and i_q are the dq-axis currents, v_{d1} and v_{q1} are the output dq-axis voltages of INV1 for the neutral point of the dc-link capacitor C_{dc1}.

The output power of INV2 is written as follows:

$$p_{INV2} = -(i_d v_{d2} + i_q v_{q2}), \tag{6}$$

where v_{d2} and v_{q2} are output dq-axis voltages of INV2 for the neutral point of the dc capacitor C_{dc2}. The dq-axis current is considered negative because the phase current is common with INV1.

From (4), (5), and (6), the power supplied to the load by the power converter is written as follows:

$$p_{out} = i_d(v_{d1} - v_{d2}) + i_q(v_{q1} - v_{q2}) = i_d v_d + i_q v_q, \tag{7}$$

where v_d and v_q are load voltages. The load dq-axis voltage is the difference between the output voltage of INV1 and INV2 from Fig. 4 and (7). In the proposed system, two voltage source inverters are connected in through the winding of the load motor. Therefore, the two inverter controls are independent, and their active or reactive output power is controlled independently. INV1 controls the single-phase ac power, and INV2 controls the power supplied to the load motor using this feature.

III. CONTROL METHOD OF PROPOSED SYSTEM

A. High Input Power Factor Control Method

The single-phase ac power is required to be pulsed at twice the power supply frequency to improve the input power factor,

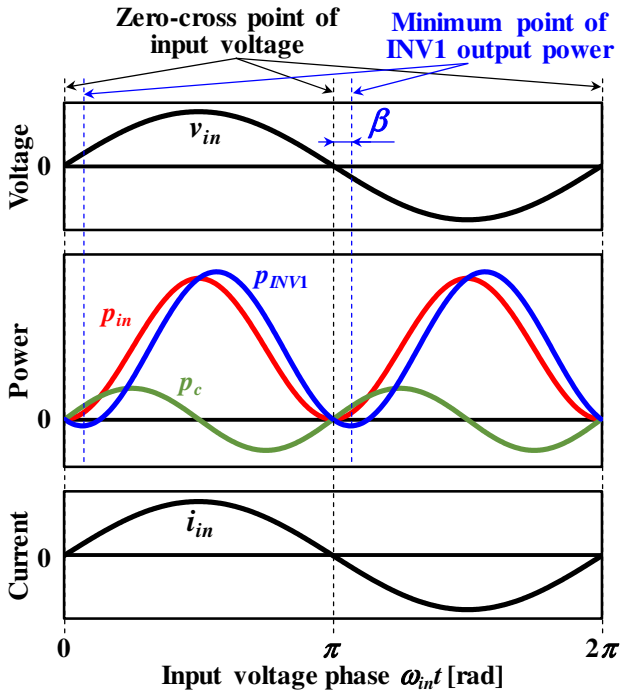

Fig. 5. Relationship between each power and single-phase ac voltage.

as with the conventional system [14]. The single-phase ac power is affected by the output power of INV1 because the proposed system shown in Fig. 3 has a small-capacity film capacitor in the dc-link. Therefore, the conventional system in [14] controls the output power of the inverter and pulsates the single-phase ac power. In the conventional control method, the output of the inverter output power controller is the q-axis reference current. Therefore, the q-axis reference current also pulsates with the pulsating reference power. Therefore, motor torque pulsation occurs. Furthermore, the conventional system requires a current controller with a high control band or repetitive control. In the proposed system, the dq-axis current must be constant to keep the torque constant.

As shown in (2) and (3), the single-phase ac power p_{in}, and the INV1 output power p_{INV1} are unequal because of the existence of the dc-link capacitor charging power p_{c1}. Fig. 5 shows the relationship between the input voltage, each power, and input current. The dc-link capacitor charging power p_{c1} is pulsated at twice the power supply frequency based on (3). Therefore, a phase difference β is generated between the single-phase ac power p_{in} and the INV1 output power p_{INV1} by this charging power. In the proposed system, the output power phase of INV1 is adjusted, and the input power factor is improved by p_{in} and v_{in}, which are in phase. If the load power p_{out} is constant, the single-phase ac power is written as follows:

$$p_{in} = p_{out} \times 2\sin^2(\omega_{in}t). \tag{8}$$

When the single-phase ac power is matched (8), the input power factor is 1 because the sinusoidal input current flows through the single-phase power supply, and the diode conduction width increases.

Here, if the pulsation component of the INV1 output power is expressed as $f(t)$; then, the output power of INV1 is written as follows:

$$p_{INV1} = p_{out} \times f(t) = i_d \times v_d f(t) + i_q \times v_q f(t), \tag{9}$$

where $f(t)$ includes the phase difference β. From (2), (3), (8) and (9), the INV1 output pulsation power component $f(t)$ is written as follows:

$$\begin{aligned} f(t) &= \frac{p_{INV1}}{p_{out}} \\ &= \frac{p_{in} - p_{c1}}{p_{out}} \\ &= 2\sin^2(\omega_{in}t) - \frac{\omega_{in} C_{dc1} {V_{inm}}^2 \sin(2\omega_{in}t)}{2p_{out}} \\ &= F_m \sin^2(\omega_{in}t + \beta) + F_o, \end{aligned} \tag{10}$$

where F_m is the maximum value of the pulsation component, and F_o is the offset component of the pulsation component. In (10), the charging power of the dc-link capacitor is considered. Therefore, the input voltage and the single-phase ac pulsating power are in phase by pulsating the output power of INV1 based on these equations. Therefore, the input power factor is approximately 1.

From (9) and (10), the dq-axis current is constant, and the output power of INV1 pulsates by pulsation the output dq-axis voltage of INV1. As shown in Fig. 5, the control method can eliminate the phase difference between the single-phase ac power p_{in} and the input voltage v_{in}. In the proposed method, the output power of INV1 is open-loop controlled because the pulsation power component is directly multiplied by the voltage reference of INV1. Therefore, the proposed control method does not require a current controller with a high control bandwidth. Additionally, the effect of the response delay is smaller than in the conventional system.

Moreover, the output pulsation power of INV1 is delayed by the delay of Digital Signal Processing (DSP) sampling and the drive circuit. The delay causes a phase difference between the single-phase ac power p_{in} and input voltage v_{in}, leading to a decrease in the input power factor. The phase of the input voltage that is output by DSP is written as follows:

$$\theta_{in\_DSP} = \omega_{in}(t - T_{delay}), \tag{11}$$

where T_{delay} is the total delay time of the control system. The phase of the input voltage calculated in the DSP is corrected as in (12) based on [13] to prevent the reduction of the input power factor by the delay time.

$$\theta_{in} = \theta_{in\_DSP} + \omega_{in} T_{delay}. \tag{12}$$

B. Suppression Control Method of Torque Pulsation

The proposed dual inverter pulsates single-phase ac power at twice the power supply frequency based on (9) and (10). Therefore, the load power and the output dq-axis voltage of INV1 pulsates. Fig. 6 shows the output voltage waveform of each inverter in the proposed system, where, the cycle of the input voltage is T_{in}. The output dq-axis voltage of INV1 is pulsated based on the single-phase ac power pulsation. In the case of the motor drive condition with only INV1, the load

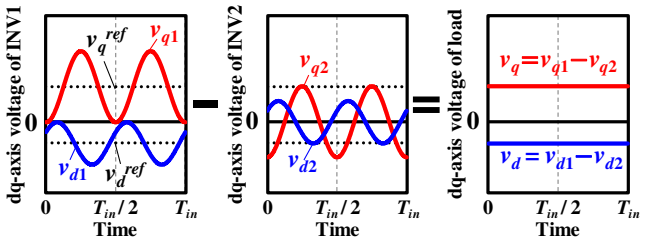

Fig. 6. Relationship between the output dq-axis voltages of each inverter and the load dq-axis voltage.

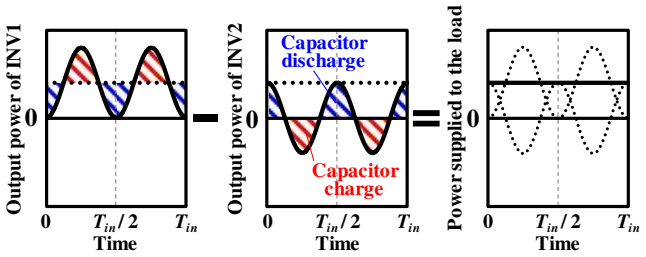

Fig. 7. Relationship between the output powers of each inverter, the load power and the state of capacitor charge or discharge.

dq-axis voltage and current pulsate to generate torque pulsation. Accordingly, INV2 outputs the voltage that compensates for the voltage pulsation of the load. The proposed system has a dual inverter, such that the load voltage can be obtained by the difference between the output voltages of INV1 and INV2 based on (1). Therefore, the load dq-axis voltages are written as follows:

$$v_d = v_{d1} - v_{d2},\ v_q = v_{q1} - v_{q2}. \tag{13}$$

Incidentally, the dq-axis voltage references v_d^{ref}, and v_q^{ref} are constant because the dq-axis currents i_d, and i_q are constant when the pulsation is suppressed. Therefore, the output dq-axis voltage reference of INV2 that compensates for the voltage pulsation is written as follows:

$$v_{d2}^{\ ref} = v_{d1} - v_d^{\ ref},\ v_{q2}^{\ ref} = v_{q1} - v_q^{\ ref}. \tag{14}$$

These equations include the INV1 output voltages v_{d1}, and v_{q1}, and have to be reproduced because the input voltage of INV1 is not constant. Therefore, the output dq-axis voltages of INV1 is reproduced using the voltage limit of the inverter. The proposed control method generates pulsating reference voltages of INV1 and compensates for the pulsation based on the output of the Auto-Current-Regulator (ACR). Therefore, INV1 and INV2 do not interfere with each other. Accordingly, the dq-axis current and torque become constant by compensating for the load dq-axis voltage to be constant.

Incidentally, the output power of each inverter has the relationship shown in (4). Fig. 7 shows each power obtained from this relationship. The INV1 output power p_{INV1} is pulsated, and the load power p_{out} is controlled to be constant by the ACR of INV1. Therefore, the INV2 output power is pulsated. The total output power of INV2 results to zero, as the pulsation is symmetric, and its average is also zero. Therefore, the charging and discharging power of the capacitor C_{dc2} are equal.

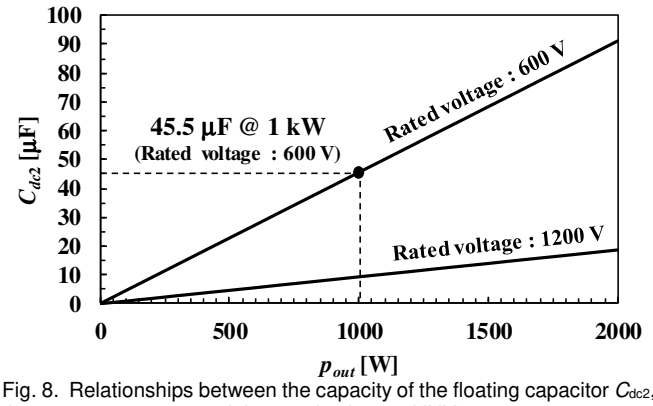

Fig. 8. Relationships between the capacity of the floating capacitor C_{dc2}, the output power p_{out} and the rated voltage of INV2.

C. Floating Capacitor Voltage Control Method

In the proposed system, the INV2 input voltage V_{dc2} must be larger than the output voltage because it compensates for the load voltage by INV2. However, V_{dc2} is exhausted, depending on the load power conditions. Based on (6), the floating capacitor C_{dc2} is in three states as follows:

$$\begin{aligned} &p_{INV2} > 0 : \text{Capacitor discharge} \\ &p_{INV2} = 0 : \text{Capacitor idle} \\ &p_{INV2} < 0 : \text{Capacitor charge.} \end{aligned} \tag{15}$$

Generally, the q-axis current i_q is controlled to be positive to generate motor torque. Therefore, the output power of INV2 becomes negative by correcting the q-axis voltage v_{q2} in the positive direction, and the capacitor is charged. In the proposed system, the load voltage pulsation that occurs at twice the power frequency is compensated by INV2. Therefore, the voltage V_{dc2} of the floating capacitor C_{dc2} pulsates at the same frequency. In the proposed system, a Band-Stop-Filter (BSF) is used to obtain the average voltage of V_{dc2}, eliminating the pulsations. The transfer function of BSF is written as follows:

$$G(s) = \frac{s^2 + \omega_o^{\ 2}}{s^2 + 2\zeta\omega_o s + \omega_o^{\ 2}},\ \omega_o = 2\pi \times 2f_{in}, \tag{16}$$

where ω_o is center angular frequency, ζ is the damping ratio and f_{in} is the single-phase ac power supply frequency. The center frequency is twice f_{in} because the INV2 input voltage V_{dc2} is pulsated at the same frequency. The damping ratio ζ removes the pulsating component of INV2 input voltage V_{dc2} by trial and error based on the simulation.

D. Determination Method of Capacitance and Voltage of Floating Capacitor

Assuming $p_c = 0$ for simplicity, the single-phase ac pulsating power is written as follows:

$$\begin{aligned} p_{in} &= V_{inm} I_{inm} \sin^2(\omega_{in} t) \\ &= \frac{1}{2} V_{inm} I_{inm} - \frac{1}{2} V_{inm} I_{inm} \cos(2\omega_{in} t) \\ &= p_{out} - p_{INV2}, \end{aligned} \tag{17}$$

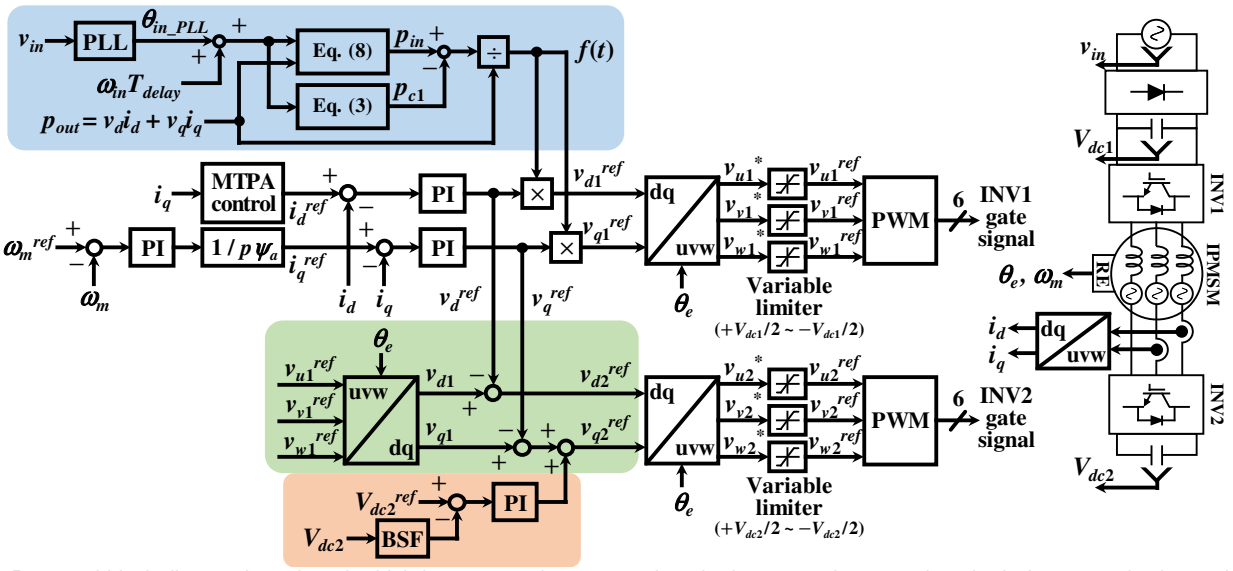

Fig. 9. Proposed block diagram based on the high input power factor control method, suppression control method of torque pulsation and input capacitor voltage control method of floating inverter.

where I_{inm} is the maximum current of the single-phase ac power supply. Based on (17), the stored energy of the floating capacitor is written as follows:

$$W_c = \int_{\frac{T}{4}}^{\frac{3T}{4}} p_{INV2}\,dt = \frac{V_{inm} I_{inm}}{2\omega_{in}} = \frac{p_{out}}{\omega_{in}}. \tag{18}$$

If the maximum value of the floating capacitor is $V_{dc2\max}$, and the minimum value is $V_{dc2\min}$, it is written as follows:

$$W_c = \frac{1}{2} C_{dc2} (V_{dc2\max}{}^2 - V_{dc2\min}{}^2). \tag{19}$$

Based on (18) and (19), the floating capacitor C_{dc2} required to suppress the load pulsation power is written as follows:

$$C_{dc2} = \frac{2 p_{out}}{\omega_{in} (V_{dc2\max}{}^2 - V_{dc2\min}{}^2)}. \tag{20}$$

From (20), the floating capacitor C_{dc2} is determined by the acceptable voltage ripple and compensating load power. Based on the maximum voltage V_{inm} of the single-phase ac power supply, and the load voltage V_a, the output voltage of INV1 is limited by the following:

$$\begin{aligned} \sqrt{\frac{2}{3}} V_{inm} &\geq 2V_a \sin^2(\omega_{in} t) \\ &= V_a - V_a \cos(2\omega_{in} t). \end{aligned} \tag{21}$$

In the proposed system, INV2 compensates for the load voltage pulsation. If the dc voltage is always larger than the output voltage of INV2, the output voltage of INV2 is limited as follows (22), based on the minimum voltage of V_{dc2}.

$$\sqrt{\frac{2}{3}} V_{dc2\min} \geq -V_a \cos(2\omega_{in} t). \tag{22}$$

From (21) and (22), the minimum value of the INV2 input voltage that enables the system to compensate for the load voltage is written as follows:

$$V_{dc2\min} \geq \frac{1}{2} V_{inm}. \tag{23}$$

From (23), $V_{dc2\min}$ is 141 V when the single-phase ac power supply voltage is 200 Vrms. Fig. 8 shows the relationship between the compensated load power and capacitor capacity. Assuming that the load power is 1 kW and the rated voltage of INV2 is 600 V (i.e., $V_{c\min}$ = 300 V), the required floating capacitor capacity is 45.5μF.

E. Proposed Control Block Diagram

Fig. 9 shows the proposed block diagram based on the high input power factor control method, suppression control method of torque pulsation, and input capacitor voltage control method of the floating inverter. The proposed control method assumes the open-end winding IPMSM load and has an automatic speed regulator. The highlighted blue part is the output pulsation power component generation block to achieve a high input power factor. The highlighted green part is the INV2 voltage reference generation block to compensate for the load voltage. The highlighted orange part is the capacitor voltage control block for compensating for a stable load voltage. First, the output voltage reference of INV1 is generated by multiplying the outputs of the dq-axis current controllers and the power pulsation. Second, the output voltage of INV1 is reproduced based on the reference voltage of INV1. Finally, the output voltage of INV2 is generated by subtracting the dq-axis reference voltage from the output dq-axis voltage of INV1, and further adding these values to the output of the voltage controller. Moreover, the reference output voltage of each inverter is limited by the variable voltage limiter using the inverters' dc voltage. The d-axis current reference is generated by Maximum Torque Per Ampere (MTPA) control.

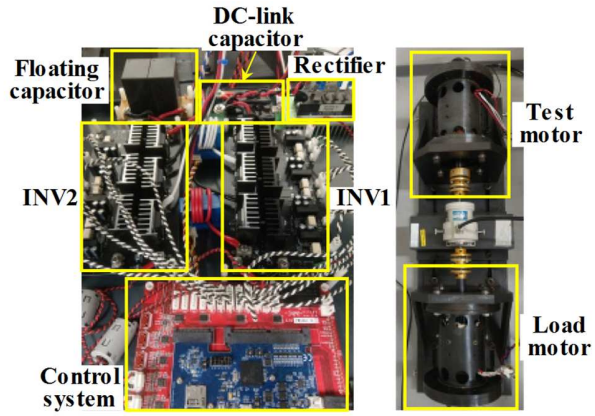

Fig. 10. Experimental setup.

TABLE II
SYSTEM AND MOTOR PARAMETERS

AC power supply voltage v_{in} and frequency f_{in}	200 Vrms and 50 Hz
Line inductance L_{in} and resistance R_{in}	0.4 mH and 0.3 Ω
DC-link capacitor C_{dc1}	12 μF
Floating capacitor C_{dc2}	50 μF
Voltage reference of floating capacitor V_{dc2}	230 V
Switching frequency f_s	10 kHz
Dead time T_d	2 μs
Bandwidth of current control system ω_c	2510 rad/s
Bandwidth of speed control system ω_s	31.4 rad/s
Proportional gain K_{vp} and integral gain K_{vi} of voltage control	2 and 10
Stator resistance R_a	0.788 Ω
dq-axis inductance L_d and L_q	10.2 mH and 20.1 mH
Linkage flux φ_a	0.137 Wb
Number of pule pairs p	2
Rated speed and torque	3000 rpm and 1.5 Nm

IV. EXPERIMENTAL RESULTS

A. Experimental Conditions

Experiments are carried out based on the proposed control method to verify the effectiveness of the motor torque pulsation suppression control. Fig. 10 shows the experimental setup. The constant torque is obtained by using a load motor connected to an electronic load. The proposed control method is implemented with a Texas Instruments TM320 floating-point digital signal processor. DL850 is used to observe each waveform, and WT3000 is used to measure the input power factor and efficiency. The system and motor parameters are listed in Table II. The dc-link capacitor C_{dc1} is defined to eliminate the inverter switching ripple. The floating capacitor C_{dc2} is defined by a determination method of the capacity and voltage of the floating capacitor. The proportional gain K_{vp} and integral gain K_{vi} of the floating capacitor voltage control are defined by trial and error based on the simulation.

B. Motor Torque Pulsation Suppression Control and High Power Factor Control Effect

Fig. 11 shows the experimental results of the conventional electrolytic capacitor-less single inverter shown in Fig. 2. In the conventional system, the q-axis current is pulsated to achieve a high input power factor. Therefore, the U-phase current is distorted because the harmonic component is superimposed on the fundamental component. Therefore, the motor torque is

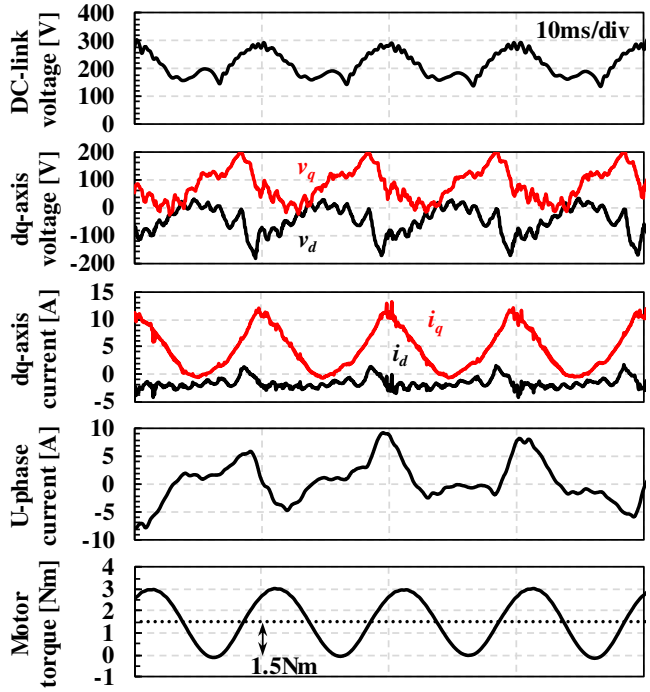

Fig. 11. Experimental results of the conventional electrolytic capacitor-less single inverter at 2500 rpm and 1.5 Nm. From top to bottom, the dc-link voltage, load dq-axis voltage, dq-axis current, U-phase current, and load motor torque.

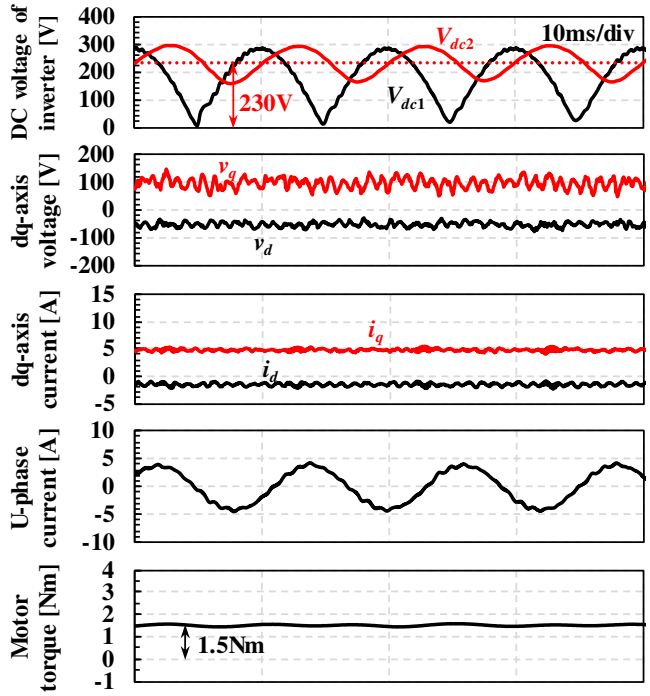

Fig. 12. Experimental results of the proposed electrolytic capacitor-less dual inverter at 2500 rpm and 1.5 Nm. From top to bottom, the dc voltage of INV1 and INV2, load dq-axis voltage, dq-axis current, U-phase current, and load motor torque.

pulsated at twice the power frequency. This torque pulsation is approximately 200% of the amplitude and generates an average torque of 1.5 Nm. The motor vibration and mechanical noise are caused depending on conditions by this torque pulsation. Fig. 12 shows the experimental results of the proposed

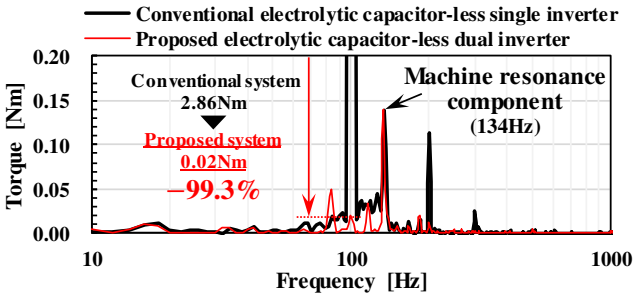

Fig. 13. FFT analysis results of motor torque in the proposed system.

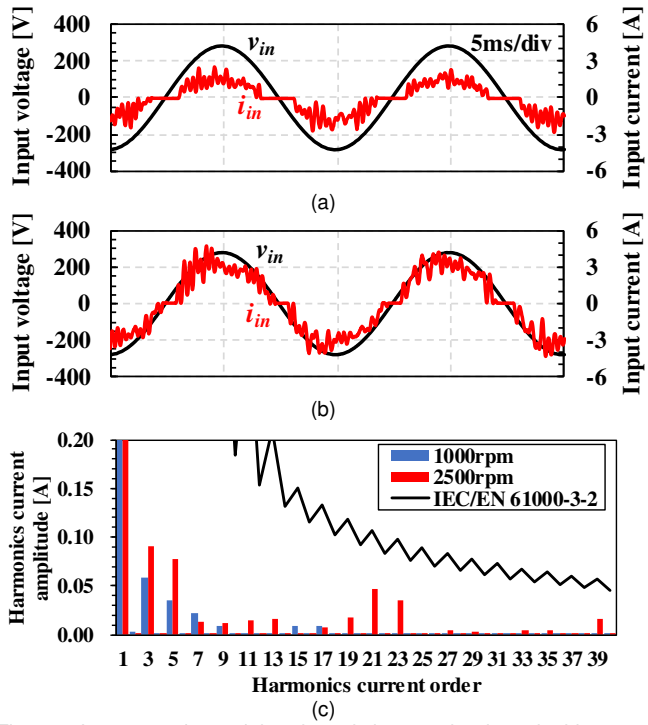

Fig. 14. Input waveform of the electrolytic capacitor-less dual inverter. (a) 1000 rpm. (b) 2500 rpm. (c) FFT analysis results of input current at each speed.

TABLE III
INPUT POWER FACTOR OF THE PROPOSED SYSTEM

Motor speed [rpm]	1000	1500	2000	2500	3000
Power Factor[%]	93.5	94.3	96.2	97.2	97.6

electrolytic capacitor-less dual inverter shown in Fig. 3. The proposed system compensates for the output dq-axis voltage pulsations of INV1 by controlling the average voltage of the floating capacitor to 230 V. As a result, the dq-axis current is constant, and the U-phase current tends to a sinusoidal waveform compared to the conventional system. Therefore, the proposed system compensates for the motor torque continuously and suppresses torque pulsation by 95.5% compared to the conventional system. Fig. 13 shows Fast Fourier Transform (FFT) analysis results of the load motor torque. In the proposed system, twice the power frequency component of the torque (i.e., 100 Hz) is reduced by 99.3%. The 134 Hz component of the torque is substantial in the conventional and proposed systems. This component is due to the mechanical resonance component of the test motor. The motor torque is pulsated with 0.14 Nm amplitude in the

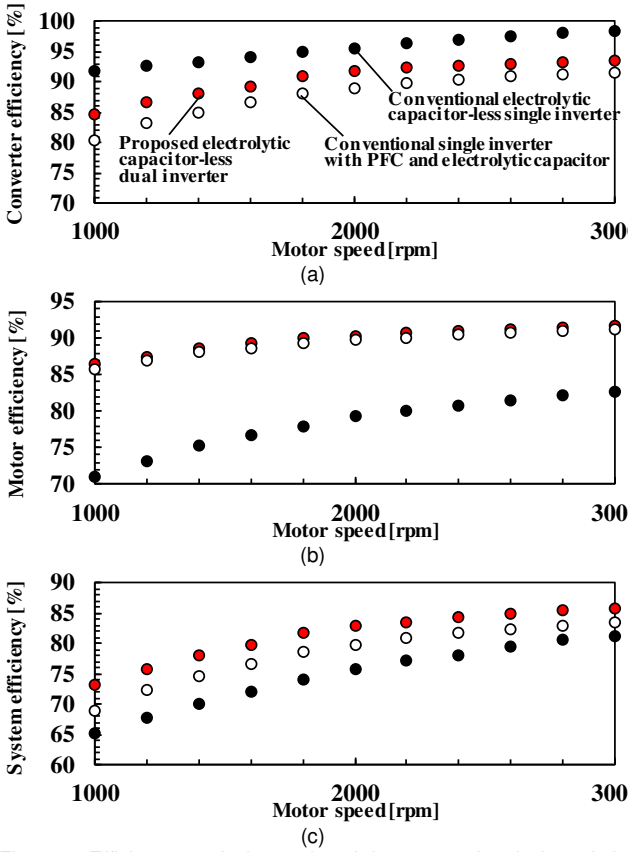

Fig. 15. Efficiency analysis results of the conventional electrolytic capacitor-less single inverter, conventional single inverter with PFC and electrolytic capacitor, and proposed electrolytic capacitor-less dual inverter at 1.5 Nm. (a) Converter efficiency. (b) Motor efficiency. (c) System efficiency.

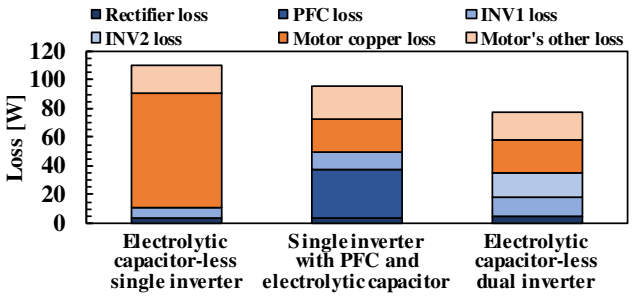

Fig. 16. Loss breakdown of the electrolytic capacitor-less single inverter, single inverter with PFC and electrolytic capacitor and electrolytic capacitor-less dual inverter.

proposed system by this mechanical resonance. The motor torque in Fig. 12 has a torque ripple of 0.19 Nm. Most of the motor torque ripple in the proposed system is the mechanical resonance component. Accordingly, the ripple shown in the torque waveform is not due to the performance of the proposed system. Fig. 14 shows the input waveform and FFT analysis results at 1000 rpm and 2500 rpm. In the proposed system, the input current feedback control is not performed. Therefore, the resonance component of the input current at approximately 2.3 kHz generated by the line inductance and the dc-link capacitance is not suppressed. Table III shows the input power factor at each speed. The input power factor is 93.5% at 1000 rpm and 97.2% at 2500 rpm. The input current of the proposed system achieves IEC/EN 61000 3-2 in all motor speed regions.

C. System Efficiency Analysis Results

Fig. 15 shows the comparison of the efficiency of the systems shown in Figs. 1, 2, and 3. Additionally, Fig. 16 shows the loss breakdown of each system at 3000 rpm, and 1.5 Nm. The copper loss of the motor is calculated based on the dc component and harmonic components of the dq-axis current. The "Motor's other loss" refers to the iron loss and mechanical loss of the test motor. Because the proposed system required two inverters, the converter efficiency is lower than that of the electrolytic capacitor-less single inverter. However, it is confirmed that it is higher than the single inverter with PFC and electrolytic capacitor because the copper loss of the boost inductor used for the PFC accounts for most of the loss. It is confirmed that the motor efficiency of the proposed system is the highest of each system. In the electrolytic capacitor-less single inverter, the copper loss of the motor is increased because the harmonic components of the motor current are increased. Furthermore, the single inverter cannot have a multi-level phase voltage compared to the dual inverter. Therefore, the iron loss of the motor in the proposed system is less than that of the conventional system. Therefore, the system efficiency of the proposed system is the highest of the three systems. Particularly, the system efficiency of the proposed system is 2.4% and 4.8% higher than that of the systems in Fig. 1 and Fig. 2, respectively.

V. Conclusion

This paper proposed power converter and control methods to realize a high input power factor and the motor suppression of the motor torque using a dual inverter without an electrolytic capacitor, and an open-end winding machine. One inverter drove the motor and the pulsating single-phase ac power, while the other suppressed the load power pulsation. The effectiveness of the proposed system was shown by experimental results with an open-end winding IPMSM load. The proposed electrolytic capacitor-less dual inverter suppressed the torque pulsation by 95.5% compared to the conventional electrolytic capacitor-less single inverter and the input power factor was 97.2% at 2500 rpm, 1.5 Nm load condition. Additionally, the system efficiency of the proposed system was 2.4% and 4.8% higher than the electrolytic capacitor-less single inverter, and single inverter with a PFC and electrolytic capacitor, respectively, because the proposed system increases the motor efficiency. Moreover, the proposed system does not require a boost inductor. Furthermore, given that the performance and cost of power devices has improved in recent years, the proposed system is expected to reduce costs further.

From these results, this paper confirmed the effectiveness of the proposed electrolytic capacitor-less inverter with a high power factor and low torque pulsation using the dual inverter and the proposed control method.

References

[1] B. Sigh, B. N. Singh, A. Chandra, K. A. Haddead, A. Pandey and D. P. Kothari, "A review of single-phase improved power quality AC-DC converters", *IEEE Trans. on Ind. Electron.*, vol. 50, DOI 10.1109/TIE.2003.817609, no. 5, pp. 962-981, Oct. 2003.

[2] O. Garcia, J. A. Cobos, R. Prieto, P. Alou and J. Uceda, "Single phase power factor correction: a survey", *IEEE Trans. on Power Electron.*, vol. 18, DOI 10.1109/TPEL.2003.810856, no. 3, pp. 749-755, May 2003.

[3] Y. Jang and M. M. Jovanovic, "Interleaved boost converter with intrinsic voltage-doubler characteristic for universal-line PFC front end", *IEEE Trans. on Power Electron.*, vol. 22, DOI 10.1109/TPEL.2007.900502, no. 4, pp. 1394-1401, Jul. 2007.

[4] H. J. Chin, Y. K. Lo, J. T. Chen and S. J. Cheng, "A high-efficiency dimmable LED driver for low-power lighting applications", *IEEE Trans. on Ind. Electron.*, vol. 57, DOI 10.1109/TIE.2009.2027251, no. 2, pp. 735-743, Feb. 2010.

[5] J. M. Alonso, J. Vina, D. G. Vaquero, G. Martinez and R. Osorio, "Analysis and design of the integrated double buck–boost converter as a high-power-factor driver for power-LED lamps", *IEEE Trans. on Ind. Electron.*, vol. 59, DOI 10.1109/TIE.2011.2109342, no. 4, pp. 1689-1697, Apr. 2012.

[6] W. Qi, S. Li, S. C. Tan and S. Y. Hui, "A single-phase three-level flying-capacitor PFC rectifier without electrolytic capacitors", *IEEE Trans. on Power Electron.*, vol. 34, DOI 10.1109/TPEL.2018.2871552, no. 7, pp.6411-6424, Jul. 2019.

[7] M. Jang and V. G. Agelidis, "A minimum power-processing-stage fuel-cell energy system based on a boost-inverter with a bidirectional backup battery storage", *IEEE Trans on Power Electron*., vol. 26, DOI 10.1109/TPEL.2010.2086490, no. 5, pp. 1568-1577, May. 2011.

[8] P. T. Krein, R. S. Balog and M. Mirjafari, "Minimum energy and capacitance requirements for single-phase inverters and rectifiers using a ripple port", *IEEE Trans on Power Electron*., vol. 27, DOI 10.1109/TPEL.2012.2186640, no. 11, pp. 4690-4698, No. 2012.

[9] I. Serban, "Power decoupling method for single-phase H-bridge inverters with no additional power electronics", *IEEE Trans. on Ind. Electron.*, vol. 62, DOI 10.1109/TIE.2015.2399274, no. 8, pp. 4805-4813, Aug. 2015.

[10] Y. Tang, Z. Qin, F. Blaabjerg and P. C. Loh, "A dual voltage control strategy for single-phase PWM converters with power decoupling function", *IEEE Trans. on Power Electron*., vol. 30, DOI 10.1109/TPEL.2014.2385032, no. 12, pp. 7060-7071, Dec. 2015.

[11] Y. Ohnuma and J. Itoh, "Space vector modulation for a single phase to three phase converter using an active buffer", in *Proc. IEEE Itn. Power Electron. Conf.*, 2010, DOI 10.1109/IPEC.2010.5543304, pp.574-580.

[12] Y. Ohnuma and J. Itoh, "A novel single-phase buck PFC AC–DC converter with power decoupling capability using an active buffer", *IEEE Trans. on Ind. Appl*., vol. 50, DOI 10.1109/TIA.2013.2279902, no. 3, pp. 1905-1914, May-Jun. 2014.

[13] H. Haga, T. Yokoyama, J. Shibata and K. Ohishi, "High power factor control for single-phase to three-phase power converter without reactor and electrolytic capacitor", in *Proc. Annu. Conf. of IEEE Ind. Electron.*, DOI 10.1109/ECCE.2009.5316050, 2008, pp. 766-771.

[14] K. Inazuma, H. Utsugi, K. Ohishi and H. Haga, "High-power-factor single-phase diode rectifier driven by repetitively controlled IPM motor", *IEEE Trans. on Ind. Electron*., vol. 60, DOI 10.1109/TIE.2012.2209610, no. 10, pp. 4427-4437, Oct. 2013.

[15] K. Abe, H. Haga, K. Ohishi and Y. Yokokura, "Fine current harmonics reduction method for electrolytic capacitor-less and inductor-less inverter based on motor torque control and fast voltage feedforward control for IPMSM", *IEEE Trans. on Ind. Electron*., vol. 64, DOI 10.1109/TIE.2016.2614270, no. 2, pp. 1071-1080, Feb. 2017.

[16] N. Zhao, G. Wang, D. Xu, L. Zhu, G. Zhang and J. Huo, "Inverter power control based on DC-link voltage regulation for IPMSM drives without electrolytic capacitors", *IEEE Trans. on Power Electron.*, vol. 33, DOI 10.1109/TPEL.2017.2670623, no. 1, pp.558-571, Jan. 2018.

[17] N. Hayashi, R. Ogawa, T. Taniguchi and M. Sekimoto, "Electrolytic capacitor-less single-phase to three-phase inverter with harmonics suppression control for air conditioner", in *Proc. Itn. Power Electron. Conf.*, 2018, DOI 10.23919/IPEC.2018.8507941, pp. 866-871.

[18] D. Pan, F. Liang, Y. Wang and T. A. Lipo, "Extension of the operating region of an IPM motor utilizing series compensation", *IEEE Trans. on Ind. Appl.*, vol. 50, DOI 10.1109/TIA.2013.2270223, no. 1, pp. 539-548, Jan.-Feb. 2014.

[19] Y. Lee and J. Ha, "Hybrid modulation of dual inverter for open-end permanent magnet synchronous motor", *IEEE Trans. on Power Electron.*, vol. 30, DOI 10.1109/TPEL.2014.2325738, no. 6, pp.3286-3299, Jun. 2015.

[20] D. Sun, Z. Zheng, B. Lin, W. Zhou and M. Chen, "A hybrid PWM-based field weakening strategy for a hybrid-inverter-driven open-winding

PMSM system", *IEEE Trans. on Energy Convers.*, vol. 32, DOI 10.1109/TEC.2017.2676020, no. 3, pp. 857-865, Sept. 2017.

Motoki Nishio received the B.E. and M.E. degrees in electrical, electronics and information engineering from the Nagaoka University of Technology, Niigata, Japan, in 2018 and 2020.
His research interests include power electronics.

Hitoshi Haga (M'08) received the B.E., M.E., and D. Eng. degrees in energy and environmental science from the Nagaoka University of Technology, Nagaoka, Japan, in 1999, 2001, and 2004, respectively. From 2004 to 2007, he was a Researcher with Daikin Industries, Ltd., Osaka, Japan. From 2007 to 2010, he was an Assistant Professor with The Sendai National College of Technology, Sendai, Japan. Since 2010, he has been with the Nagaoka University of Technology, where he became an Associate Professor in 2016. His research interests include power electronics.